Polymer Journal (2019) 51:257–263
https://doi.org/10.1038/s41428-018-0137-4

ORIGINAL ARTICLE

Fabrication and characterization of elastomeric semiconductive thiophene polymers by peroxide crosslinking

Jian Shen[1] · Iori Sugimoto[1] · Takuya Matsumoto[1] · Shohei Horike[1] · Yasuko Koshiba[1] · Kenji Ishida[1] · Atsunori Mori[1] · Takashi Nishino[1]

Received: 19 July 2018 / Revised: 15 September 2018 / Accepted: 18 September 2018 / Published online: 17 October 2018

Abstract

In this study, semiconductive elastomers composed of homopolythiophene with disiloxane moieties were developed. The crosslinked molecular structure in the polythiophene elastomers was introduced by dicumyl peroxide, one of the typical peroxide crosslinking reagents. The elastomers were produced through a hot-pressing process above the melting point of the polythiophene. Stress–strain curves that included tensile tests and cycle loading–unloading tests defined the crosslinked polythiophenes as elastomers. Their electrical conductivities were evaluated by two-point measurements under nondeformation and uniaxial deformation states. The results indicated that the concentration of crosslinking reagents greatly influenced the mechanical and electrical properties of crosslinking polymers. With the addition of the crosslinking reagent in concentrations from 2.5 phr to 10.0 phr, elongation at break decreased largely from 95% to 51%, while excellent elastic recoveries were observed. In the electrical resistivity measurements, all the crosslinking polymers possessed high stability of electrical properties against elongation.

Introduction

Conjugated polymers, such as regioregular poly(3-alkyl thiophene)s [1, 2] and their copolymers and composites [3, 4], present comparatively high electrical conductivity and high field-effect mobility in doped states [5]. In recent years, they have contributed to the development of electrical devices such as photovoltaic cells [6], batteries [7], capacitors [8], and transistors [9]. As semiconductive polymers have advantages such as low cost, light weight, excellent processability, and moldability, they have attracted attention in the field of materials science and the electrical industry [10, 11]. These developments and acceptance have attracted much attention to next-generation flexible and stretchable devices. Therefore, in these devices, not only high electrical and optical properties but also robust mechanical performance is desired. The mechanical properties of semiconductive polymers are significant factors in the application of sheet-type organic solar cells [12], flexible displays [13], wearable electronic devices [14], and any other polymer-based semiconductors. For the improvement of durability and the expansion of applications, polymer materials with high flexibilities and tensile properties are indispensable. Therefore, these polymer materials enable us to design the comparable long-life electrical devices against mechanical deformation and fracture, such as stretching, distortion, and bending [15–18].

The use of elastomer composites with inorganic fillers is one of the conventional methods for flexible electrical conductive materials. They are produced by mixing the electrically conductive fillers with nonconductive elastomers in the molten states, using a batch mixer or a molding compounder. Fillers such as carbon black, metal particles, and metal-coated inorganic particles are used in the conductive composites. Glass particles coated with silver and nickel-coated graphite are suggested as fillers for their high electrical functionality in composites [19]. Thermoplastic elastomers such as polyurethane [20] and

Electronic supplementary material The online version of this article (https://doi.org/10.1038/s41428-018-0137-4) contains supplementary material, which is available to authorized users.

✉ Takashi Nishino
tnishino@kobe-u.ac.jp

[1] Department of Chemical Science and Engineering, Graduate School of Engineering, Kobe University, Rokko, Nada, Kobe 657-8501, Japan

polydimethylsiloxane [21] are used as matrix materials. The conductive paths caused by percolation between fillers lead to high electrical conductivity. For high conductivity, large amounts of fillers loaded in composites are required, while the excessive amounts of filling materials account for mechanical defects of the composites [20, 22]. Moreover, deforming and stretching of electrical devices disconnect conductive paths in their composites, and these actions are associated with a significant decrease in electrical conductivity [21, 23]. For high mechanical durability, electrically conductive polymers with single components are desired.

In recent years, stretchability in semiconductive polymers has been achieved by modification of the molecular structure by introducing chemical crosslinking groups or by surface embedding in an elastomer [24]. These stretchable elastic polymers restrict the running condition of electrical devices and the structure of device systems. Electrical conductive elastomers are a promising material for the development of wearable devices because of the properties of deformability, shock resistance, chemical resistivity, and light weight [25, 26].

In our previous work, we synthesized the thiophene polymer with disiloxane moieties on its side chains (P3SiT) [27, 28]. The synthesized polymer showed high molecular weight and highly regioregular molecular structure. P3SiT performed well with respect to dissolubility in organic solvent, high mechanical flexibility (over 200% of elongation at break), and semiconductive electrical performance [29–33]. Herein, we controlled the structure of molecular chains of P3SiT through peroxide crosslinking for high elastic recovery of the polymer. Owing to a glass transition temperature lower than room temperature, introduction of chemical crosslinking provided high elasticity (i.e., high elastic recovery). Therefore, we investigated the electric properties of crosslinked polythiophenes as well as their mechanical properties and structure through cycling loading–unloading tests and X-ray diffraction measurements with synchrotron radiation at SPring-8 BL03XU.

Experimental section

Regioregular poly(3-substituted thiophene) with siloxane moieties on its side chain (P3SiT) was prepared by polymerization of 2-bromo-3-substituted-thiophene with siloxane moieties, as in the reported method [28, 29]. The synthesized P3SiT showed a weight-average molecular weight of 100k and a molecular weight distribution of 1.30.

The crosslinking of P3SiT was performed using dicumyl peroxide (DCP) as the crosslinking reagent above the melting point of P3SiT ($T_m = 142$ °C) [34]. DCP and 2.0 wt % P3SiT (0.10 versus 5 g chloroform) were dissolved into chloroform, and the solution was casted on a PTFE Petri dish. After the solvent was removed for 48 h at room temperature, P3SiT-DCP cast films with dimensions of 40 mm × 40 mm × 60 μm were obtained. The degree of crosslinking was controlled by the DCP concentration (2.5, 5.0, 7.5, and 10.0 phr). The P3SiT cast films were heated under 10 MPa pressure for 15 min at 150 °C and then for 5 min at 180 °C. Finally, they were quenched by cold water immediately and dried up. To maintain the flatness of the surfaces, both sides of the cast film surfaces of the PTFE sheets were subjected to hot pressing.

Fourier transform infrared (FT-IR) absorption measurements were performed with an FT-IR microscope (IRTracer-100, AIM-9000; Shimazu. Co. Ltd.) in the transmittance mode. Two-dimensional X-ray diffraction measurements were performed on a synchrotron radiation accelerator at SPring-8 BL03XU (wavelength of X-ray beam: 1.0 Å; camera length: 0.60 m) with a Pilatus3 1M detector (Dectris), and the exposure time was 1.0 s. The X-ray diffraction measurement (XRD) was performed with symmetrical reflection geometry and Cu Kα radiation (RINT 2000; Rigaku). The X-ray beam was generated at 40 kV, 20 mA. Differential scanning calorimetry (DSC) profiles were recorded on a Rigaku DSC8230 with a scan rate of 10 °C/min under dried nitrogen. Dynamic mechanical analysis was performed on a DVA-200 instrument (itk Co. Ltd.) in tensile mode, and the storage modulus, the loss modulus, and the mechanical tanδ of the P3SiT samples were determined as a function of temperature. The initial lengths were 20 mm, and the thicknesses were 60 μm. The maximum strain was 150%, and the frequency was 2 Hz. In tensile tests, an Autograph AG-X plus (Shimadzu Co. Ltd) was used for investigating the mechanical performance of crosslinked P3SiT. The tensile test samples were trimmed to dimensions of 40 mm × 5 mm (half the size of the grabbing part) and were tensiled at the speed of 5 mm/min. Cycling tests were also performed by the tensile testing machine. The loading strain at first setting was 10%, and it was back to 0% immediately. Then, the value of the next loading strain was increased by 10 points relative to the previous strain. The strain history was from 0, 10, 0, 20, 0, 30%, etc. The electrical resistance of crosslinked P3SiT films was measured in ambient atmosphere by two-point measurements using a Keysight Technologies B1500A with voltage ranges of −30 to 30 V. VEC-40K (Ayumi-ind) was utilized to deposit Au electrodes onto polymer cast film surfaces under vacuum. The gaps between electrodes with a length of 30 mm were 110 μm on average, and the thicknesses of the electrodes were controlled to be 200 nm. The electrical resistivity (R) of these samples as a function of voltage was calculated by Ohm's law. The average values in the range of the electrical resistivity plateau were employed as the experimental results of these samples.

Scheme 1 Crosslinking of P3SiT with DCP

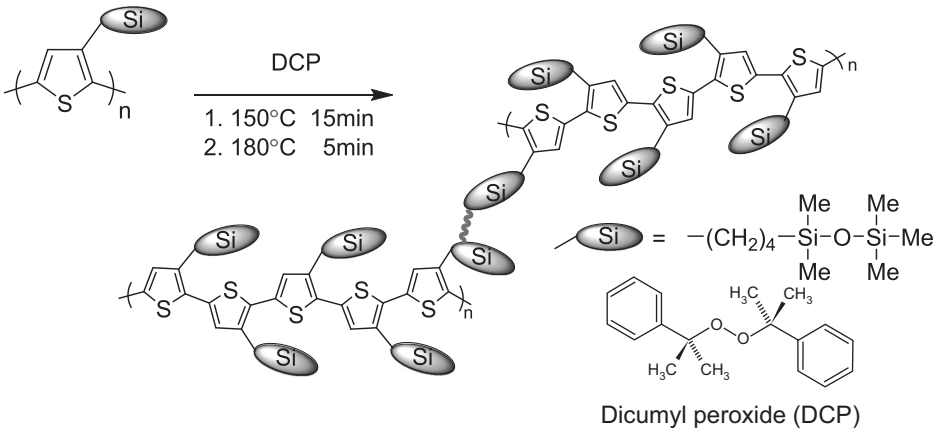

Results and discussion

High-molecular-weight regioregular poly(3-substitude thiophene) with siloxane moieties (P3SiT) was polymerized by the Kumada coupling reaction based on a nickel(II) catalyst [28, 35], and cast P3SiT was crosslinked by hot pressing with various amounts of DCP crosslinking reagents, as shown in Scheme 1. Crosslinked P3SiTs were insoluble in chloroform and any other common organic solvents, which were good solvents for P3SiT, as shown in Figure S1 in the Supporting Information. The degree of swelling of crosslinked P3SiT with chloroform for 48 h at room temperature was evaluated. The results are shown in Table S1 in the Supporting Information. The high concentration led to the lower degree of swelling. In addition, FT-IR measurements of P3SiT with or without crosslinks were performed in order to investigate changes in the chemical structure. From the FT-IR spectra in Figure S2, the chemical structure of the main chains of P3SiT remained. These results suggested that the intermolecular crosslinks of P3SiT were constructed.

In our previous works [29], we have reported that P3SiT with more than 200% tensile elongation before fracture was a crystalline polymer, an observation that was based on X-ray diffraction measurements, as shown in Figure S3 in the Supporting Information. To investigate the crystallinity of crosslinked P3SiTs, we evaluated X-ray diffraction photographs of crosslinked P3SiT with synchrotron radiation at SPring-8 BL03XU. The X-ray diffraction photographs are shown in Fig. 1. In the photographs of all the undrawn crosslinked P3SiTs, Debye–Scherrer rings originating from (100) planes were observed. These mean that even after crosslinking, slight amounts of P3SiT crystallites were maintained. As the degrees of crosslinking were increased, the Debye–Scherrer rings were distracted. Their profiles are shown in Fig. 2. Compared with noncrosslinked P3SiT, much weaker and broader diffraction peaks originating from 100 reflection was observed at $2\theta = 4.3°$ in the profiles of crosslinked P3SiTs. However, the shift of the 2θ angles of the 100 reflection by crosslinking was quite small. These results also supported that the crystalline structure of P3SiT was partially destroyed by the crosslinking process, but the crystal structural lattice itself remained unchanged. Therefore, in the DSC thermograms of the crosslinked P3SiT in Figure S5 in the Supporting Information, the melting peak areas were decreased, and the temperature became lower with increasing DCP concentration. In addition, the crystallite size was evaluated from Scherrer's equation, and the data are shown in Table S2 in the Supporting Information. The crystallite size of crosslinked P3SiT with various DCP concentrations tended to decrease.

Figure 3 shows the temperature dependence of the storage modulus (E'), the loss modulus (E''), and the mechanical loss tangent (tanδ) of crosslinked P3SiTs. The broader peaks of the tanδ curves resulted from primary transitions of molecular chains accompanied by large drops in the storage modulus. Several factors are considered to contribute to these broadenings, such as inhibition of molecular motions by crosslinking and reduction of crystallinity. As a result, their T_g values were observed at around -2 °C, which were higher than that without crosslinking ($T_g = -10$ °C). The glass transition temperatures (T_g) of crosslinked P3SiTs with various DCP concentrations are shown in Table S3 in the Supporting Information. Nevertheless, even after crosslinking, all the T_g values of the crosslinked P3SiTs were still much lower than room temperature, which suggests the polymers remained in the rubber state at room temperature. The E' of crosslinked P3SiT at room temperature decreased with the addition of DCP. This is because the formation of the crosslinked structure decreased the crystallinity of the P3SiTs, which would make the crosslinked P3SiTs more elastic. The crystallites of P3SiT took a dominant role in controlling the mechanical properties. Therefore, the mechanical behavior of the crosslinked P3SiTs was different from the conventional rubbers comprised of amorphous polymers.

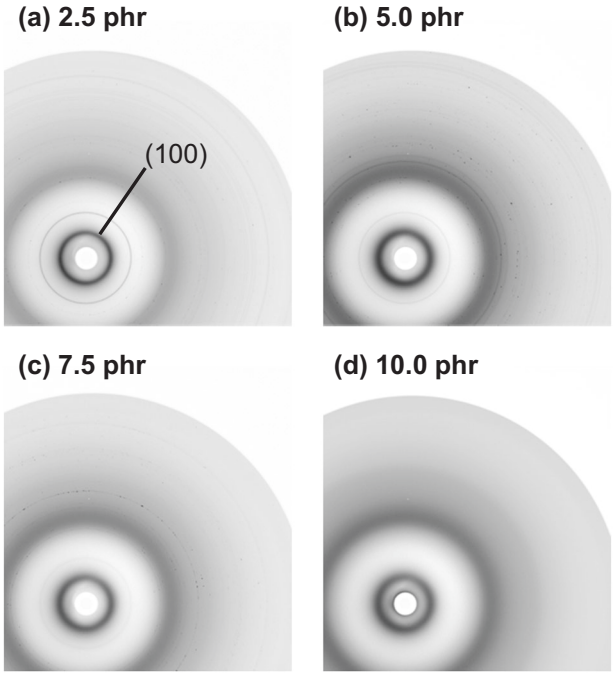

Fig. 1 X-ray diffraction photographs of crosslinked P3SiTs with various DCP concentrations

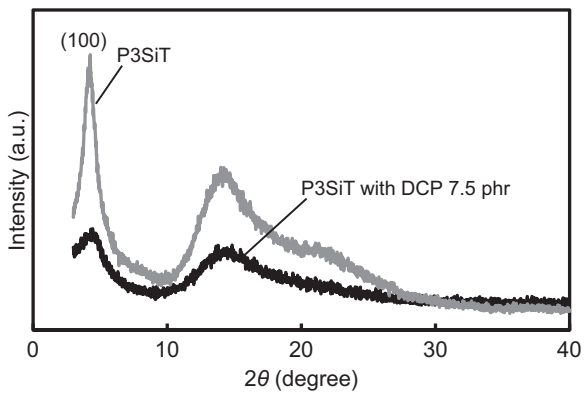

Fig. 2 X-ray diffraction profiles of P3SiT (gray) and crosslinked P3SiT (black) with DCP (7.5 phr)

The stress–strain curves of crosslinked P3SiTs with different DCP concentrations are shown in Fig. 4. Introduction of crosslinks made the Young's modulus (E), the tensile strength (σ_{max}), and the elongation at break (ε_{max}) of the crosslinked P3SiTs lower compared with those of the P3SiT before crosslinking, as shown in Table 1. As described above, these results were attributed to the lowering of crystallinity through crosslinking. The addition of crosslinking reagents restricted the tensile strength and the elongation of the crosslinked P3SiTs. In contrast, the high degree of crosslinking provided not only a lower Young's modulus but also the disappearance of yielding points. Even in the crosslinked P3SiT with the minimum DCP concentration (2.5 phr), the tensile fracture occurred at 95% elongation. When the addition of DCP was up to 10.0 phr, the elongation at break was down to 50%. These elongations were much larger compared with that of poly(3-hexylthiophene) (P3HT), which has been accepted as a conventional hole transfer electronic material in organic devices. This comparison suggested that P3SiT, even after crosslinking, possessed enough potential in flexibility and stretch properties.

To further investigate the elastomeric performance of crosslinked P3SiTs, we measured their repeated loading–unloading tensile tests. These results are represented in Fig. 5 and Figure S6 in the Supporting Information. P3SiT demonstrated high elastic recovery only below 10% of the tensile strain and completely lost that over 50% [29], whereas crosslinked P3SiTs maintained high elastic recoveries until broken because of their crosslinked molecular structure. The elastic recovery was 40% for P3SiT with 2.5 phr DCP after 90% strain. Moreover, that with DCP 10.0 phr was nearly 0% even after 40% strain. Thus, the crosslinked P3SiT with 10.0 phr DCP showed almost perfect recovery every time after loading. These results suggest that introduction of chemical crosslinking is a reasonable method for achievement of high elasticity and recovery in polythiophene derivatives.

Crosslinked P3SiT films with Au electrodes were prepared, and the current–voltage curves were obtained by two-point measurements. We investigated the influence of crosslinking and mechanical deformation on the electrical properties of the elastomeric crosslinked P3SiTs, which were composed of only thiophene homopolymer. In Table 2, we summarize the electrical resistivity (R) and sheet resistivity (R_s) of crosslinked P3SiTs with various DCP concentrations and mechanical states. We measured current–voltage curves of samples in nondeformation states and approximately 50% elongated states. The samples in nondeformation or elongation states were fixed on silicon wafers before deposition of Au electrodes on surfaces. Measurements of the elongated samples were carried out in the direction parallel to elongation. We failed to measure the conductivity of crosslinked P3SiTs with 10.0 phr in elongation states: the sample could not maintain a mechanical steady state, and it cracked after vapor deposition. The electrical conductivities of crosslinked P3SiTs showed a decreasing tendency with the addition of DCP. The R_s values of samples with DCP concentration were from 10^2 to 10^5 times higher than that of the noncrosslinked one. This could be attributed to the formation of intermolecular crosslinks and lower crystallinity. Therefore, we have considered that the higher crystallinity and control of crosslinking in P3SiTs could improve their electric properties. Moreover, compared to the reported conductive polymer materials and composites [36–38], the electrical resistance remained relatively constant with or without

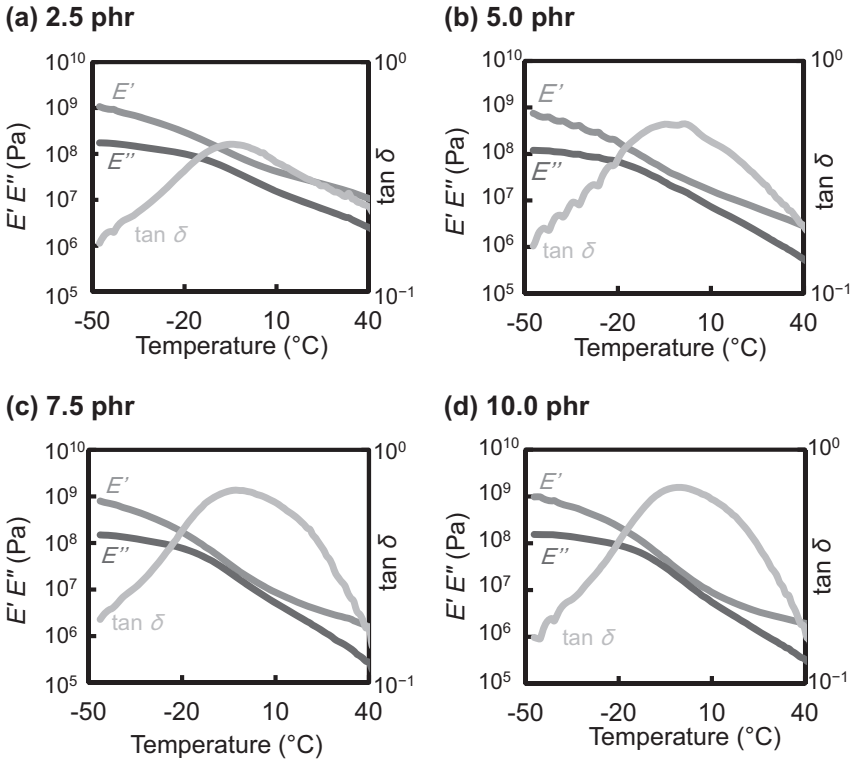

Fig. 3 Relationship between storage, loss modulus, and mechanical tan δ of crosslinked P3SiTs with different DCP concentrations and temperature

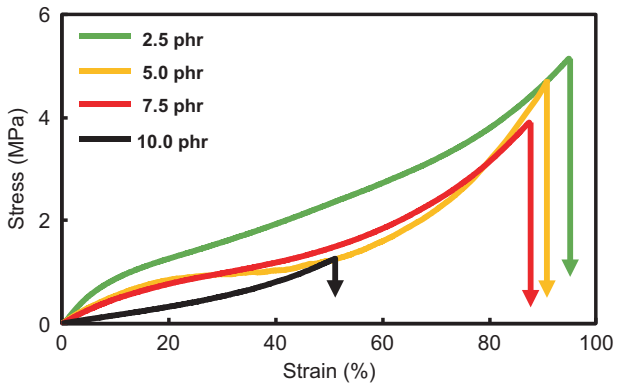

Fig. 4 Stress–strain curves of crosslinked P3SiTs with different DCP concentrations: 2.5 phr (green), 5.0 phr (yellow), 7.5 phr (red), and 10.0 phr (black)

Table 1 Mechanical properties of cast and crosslinked P3SiTs with various DCP concentrations

DCP concentration (phr)	E (MPa)	σ_{max}(MPa)	ε_{max}(%)
0[a]	43.0	6.0	226
2.5	13.1	5.1	95
5.0	7.0	4.7	91
7.5	5.9	3.9	87
10.0	1.8	1.3	51

[a]Ref. [6]

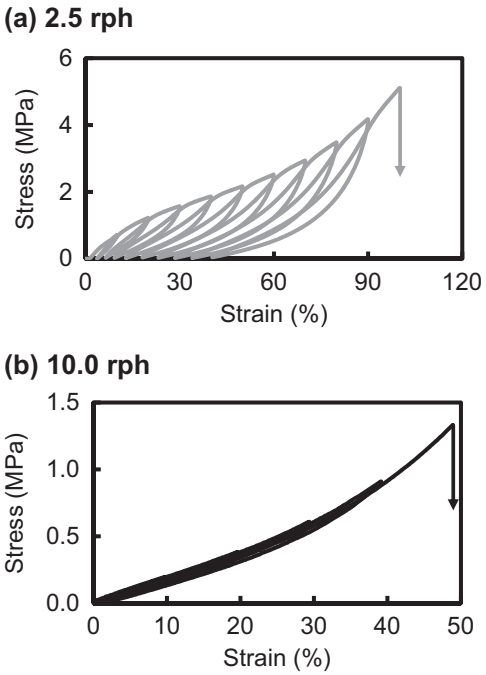

Fig. 5 Stress–strain curves of cycling loading–unloading tests of crosslinked P3SiTs with DCP concentration of (**a**) 2.5 phr and (**b**) 10.0 phr

mechanical elongation. Owing to their thiophene-only composition, mechanical deformation had little influence on electrical conductive paths in crosslinked P3SiTs.

Table 2 Resistivity of crosslinked P3SiTs with various DCP concentrations under 0 and 50% elongation

DCP concentration (phr)	$R(\Omega)$	$R_s(\Omega$/square)
0 (normal) [a]	6.2×10^4	1.8×10^4
0 (3 times drawn) [a]	4.0×10^4	1.1×10^4
2.5 (0% elongation)	4.6×10^6	1.3×10^8
2.5 (50% elongation)	5.4×10^7	1.5×10^9
5.0 (0% elongation)	6.8×10^9	1.9×10^{11}
5.0 (50% elongation)	6.8×10^9	1.9×10^{11}
7.5 (0% elongation)	4.8×10^9	1.3×10^{11}
7.5 (50% elongation)	5.0×10^9	1.4×10^{11}
10.0 (0% elongation)	4.3×10^9	1.2×10^{11}
10.0 (50% elongation)	No data [b]	No data [b]

[a]Ref. [6]

[b]Crosslinked P3SiT with 10 phr DCP concentration was broken at 50% elongation

Conclusions

We synthesized peroxide-crosslinked thiophene polymers by hot pressing, using DCP as the reagent. The weak peaks assigned to the (100) plane emerged by X-ray diffraction profiles. However, the inherent crystalline structure of P3SiT mostly disappeared by the introduction of crosslinks. Therefore, crosslinked P3SiT showed a lower Young's modulus ($E = 1.8$–13.1 MPa) but larger elongation at break ($\varepsilon_{max} = 51$–95%) relative to P3HT, and it showed greater elastic recovery compared to that of the noncrosslinked one. Crosslinking brought P3SiT higher elasticity in mechanical properties. The crosslinked P3SiT presented steady electrical properties against mechanical deformation. Peroxide crosslinking is indicated to be a desirable method to control mechanical properties of thiophene polymers, and crosslinked polythiophene elastomers are promising materials in flexible organic solar cells and wearable devices.

Funding This work was supported by a Grant-in-Aid for Scientific Research on Innovative Areas "New Polymeric Materials Based on Element-Blocks (No.2401)" (24102009) of the Ministry of Education, Culture, Sports, Science, and Technology, Japan. The synchrotron radiation experiments were performed at the BL03XU of SPring-8 with the approval of the Japan Synchrotron Radiation Research Institute (JASRI) (Proposal No. 2015A7210, 2015B7260, 2016A7210, and 2016B7260).

Compliance with ethical standards

Conflict of interest The authors declare no competing financial interest.

References

1. Dang MT, Hirsch L, Wantz G, Wuest JD. Controlling the morphology and performance of bulk heterojunctions in solar cells. Lessons learned from the benchmark poly(3-hexylthiophene): [6,6]-phenyl-C61-butyric acid methyl ester system. Chem Rev. 2013;113:3734–65.
2. Malik S, Nandi AK. Crystallization mechanism of regioregular poly(3-alkyl thiophene)s. J Polym Sci Part B Polym Phys. 2002;40:2073–85.
3. Ahmed E, Kim FS, Xin H, Jenekhe SA. Benzobisthiazole–thiophene copolymer semiconductors: synthesis, enhanced stability, field-effect transistors, and efficient solar cells. Macromolecules. 2009;42:8615–8.
4. Yan H, Huang Y. Polymer composites of carbon nitride and poly (3-hexylthiophene) to achieve enhanced hydrogen production from water under visible light. Chem Commun. 2011;47:4168–70.
5. Bao Z, Dodabalapur A, Lovinger AJ. Soluble and processable regioregular poly(3-hexylthiophene) for thin film field-effect transistor applications with high mobility. Appl Phys Lett. 1996;69:4108–10.
6. Li G, Zhu R, Yang Y. Polymer solar cells. Nat Phot. 2012;6:153–61.
7. Oschmann B, Park J, Kim C, Char K, Sung YE, Zentel R. Copolymerization of polythiophene and sulfur to improve the electrochemical performance in lithium-sulfur batteries. Chem Mater. 2015;27:7011–7.
8. Raja M, Lloyd GCR, Sedghi N, Eccleston W, Di Lucrezia R, Higgins SJ. Conduction processes in conjugated, highly regioregular, high molecular mass, poly(3-hexylthiophene) thin-film transistors. J Appl Phys. 2002;92:1441–5.
9. Mallik AB, Locklin J, Mannsfeld SCB, Reese C, Roberts ME, Senatore ML et al. Organic field-effect transistors. Adv Mater. 1998;4095:159.
10. Brabec CJ, Sariciftci NS, Hummelen JC. Plastic solar cells. Adv Funct Mater. 2001;11:15–26.
11. Coakley KM, McGehee MD. Conjugated polymer photovoltaic cells. Chem Mater. 2004;16:4533–42.
12. Lipomi DJ, Tee BCK, Vosgueritchian M, Bao Z. Stretchable organic solar cells. Adv Mater. 2011;23:1771–5.
13. Leterrier Y, Médico L, Demarco F, Månson JAE, Betz U, Escolà MF et al. Mechanical integrity of transparent conductive oxide films for flexible polymer-based displays. Thin Solid Films. 2004;460:156–66.
14. Zeng W, Shu L, Li Q, Chen S, Wang F, Tao XM. Fiber-based wearable electronics: a review of materials, fabrication, devices, and applications. Adv Mater. 2014;26:5310–36.
15. Cho CK, Hwang WJ, Eun K, Choa SH, Na SI, Kim HK. Mechanical flexibility of transparent PEDOT:PSS electrodes prepared by gravure printing for flexible organic solar cells. Sol Energy Mater Sol Cells. 2011;95:3269–75.
16. Oliva-Avilés AI, Avilés F, Sosa V. Electrical and piezoresistive properties of multi-walled carbon nanotube/polymer composite films aligned by an electric field. Carbon. 2011;49:2989–97.
17. Na S-I, Kim S-S, Jo J, Kim D-Y. Efficient and flexible ITO-free organic solar cells using highly conductive polymer anodes. Adv Mater. 2008;20:4061–7.
18. Rowell MW, Topinka MA, McGehee MD, Prall HJ, Dennler G, Sariciftci NS et al. Organic solar cells with carbon nanotube network electrodes. Appl Phys Lett. 2006;88:2–5.
19. Karttunen M, Ruuskanen P, Pitkänen V, Albers WM. Electrically conductive metal polymer nanocomposites for electronics applications. J Electron Mater. 2008;37:951–4.
20. Mi HY, Li Z, Turng LS, Sun Y, Gong S. Silver nanowire/thermoplastic polyurethane elastomer nanocomposites: thermal, mechanical, and dielectric properties. Mater Des. 2014;56:398–404.
21. Amjadi M, Pichitpajongkit A, Lee S, Ryu S, Park I. Highly stretchable and sensitive strain sensor based on silver-elastomer nanocomposite. ACS Nano. 2014;8:5154–63.

22. Larmagnac A, Eggenberger S, Janossy H, Vörös J. Stretchable electronics based on Ag-PDMS composites. Sci Rep. 2014;4:1–7.
23. Liang J, Li L, Chen D, Hajagos T, Ren Z, Chou SY, et al. Intrinsically stretchable and transparent thin-film transistors based on printable silver nanowires, carbon nanotubes and an elastomeric dielectric. Nat Commun. 2015;6:7647.
24. Rodriquez D, Kim J-H, Root SE, Fei Z, Boufflet P, Heeney M et al. Comparison of methods for determining the mechanical properties of semiconducting polymer films for stretchable electronics. ACS Appl Mater Interfaces. 2017;9:8855–62.
25. Le VT, Kim H, Ghosh A, Kim J, Chang J, Vu QA et al. Coaxial fiber supercapacitor using all-carbon material electrodes. ACS Nano. 2013;7:5940–7.
26. Meng Y, Zhao Y, Hu C, Cheng H, Hu Y, Zhang Z et al. All-graphene core-sheath microfibers for all-solid-state, stretchable fibriform supercapacitors and wearable electronic textiles. Adv Mater. 2013;25:2326–31.
27. Tamba S, Fuji K, Meguro H, Okamoto S, Tendo T, Komobuchi R et al. Synthesis of high-molecular-weight head-to-tail-type poly(3-substituted-thiophene)s by cross-coupling polycondensation with [CpNiCl(NHC)] as a catalyst. Chem Lett. 2013;42:281–3.
28. Fujita K, Sumino Y, Ide K, Tamba S, Shono K, Shen J et al. Synthesis of poly(3-substituted thiophene)s of remarkably high solubility in hydrocarbon via nickel-catalyzed deprotonative cross-coupling polycondensation. Macromolecules. 2016;49:1259–69.
29. Jian S, Keisuke F, Takuya M, Chizuru H, Masahiro M, Kenji I et al. Mechanical, thermal, and electrical properties of flexible polythiophene with disiloxane side chains. Macromol Chem Phys. 2017;218:1700197.
30. Han AR, Lee J, Lee HR, Lee J, Kang SH, Ahn H et al. Siloxane side chains: a universal tool for practical applications of organic field-effect transistors. Macromolecules. 2016;49:3739–48.
31. Lee EK, Park CH, Lee J, Lee HR, Yang C, Oh JH. Chemically robust ambipolar organic transistor array directly patterned by photolithography. Adv Mater. 2017;29:1605282.
32. Lee J, Han AR, Kim J, Kim Y, Oh JH, Yang C. Solution-processable ambipolar diketopyrrolopyrrole-selenophene polymer with unprecedentedly high hole and electron mobilities. J Am Chem Soc. 2012;134:20713–21.
33. Lee J, Han AR, Yu H, Shin TJ, Yang C, Oh JH. Boosting the ambipolar performance of solution-processable polymer semiconductors via hybrid side-chain engineering. J Am Chem Soc. 2013;135:9540–7.
34. Suyama S, Ishigaki H, Watanabe Y, Nakamura T. Crosslinking of polyethylene by dicumyl peroxide in the presence of 2,4-diphenyl-4-methyl-1-pentene. Polym J. 1995;27:371–5.
35. Hu X. Nickel-catalyzed cross coupling of non-activated alkyl halides: a mechanistic perspective. Chem Sci. 2011;2:1867.
36. Görrn P, Cao W, Wagner S. Isotropically stretchable gold conductors on elastomeric substrates. Soft Matter. 2011;7:7177–80.
37. Tait JG, Worfolk BJ, Maloney SA, Hauger TC, Elias AL, Buriak JM et al. Spray coated high-conductivity PEDOT:PSS transparent electrodes for stretchable and mechanically-robust organic solar cells. Sol Energy Mater Sol Cells. 2013;110:98–106.
38. Flandin L, Chang A, Nazarenko S, Hiltner A, Baer E. Effect of strain on the properties of an ethylene-octene elastomer with conductive carbon fillers. J Appl Polym Sci. 2000;76:894–905.